A Journal of the Gesellschaft Deutscher Chemiker
Angewandte
GDCh
International Edition
Chemie
www.angewandte.org

Accepted Article

Title: Amplified Self-Immolative Release of Small Molecules by Spatial Isolation of Reactive Groups on DNA-Minimal Architectures

Authors: Hanadi Farouk Sleiman, Alexander Prinzen, Daniel Saliba, Christopher Hennecker, Trinh Tuan, and Anthony Mittermaier

To be cited as: *Angew. Chem. Int. Ed.* 10.1002/anie.202001123

Link to VoR: https://doi.org/10.1002/anie.202001123

WILEY-VCH

10.1002/anie.202001123

WILEY-VCH

RESEARCH ARTICLE

Amplified Self-Immolative Release of Small Molecules by Spatial Isolation of Reactive Groups on DNA-Minimal Architectures

Alexander L. Prinzen, Daniel Saliba, Christopher Hennecker, Tuan Trinh, Anthony Mittermaier and Hanadi F. Sleiman*

Abstract: Triggering the release of small molecules in response to unique biomarkers is important for applications in drug delivery and biodetection. Due to typically low quantities of biomarker, amplifying release is necessary to gain appreciable responses. Nucleic acids have been used for both their biomarker recognition properties and as stimuli, notably in amplified small molecule release via nucleic acid-templated catalysis (NATC). The multiple components and reversibility of NATC, however, make it difficult to apply *in vivo*. Here, we report the first use the hybridization chain reaction (HCR) for the amplified, conditional release of small molecules from standalone nanodevices. We first couple HCR with a DNA-templated reaction resulting in the amplified, immolative release of small molecules. Moreover, we integrate the HCR components into single nanodevices as DNA tracks and spherical nucleic acids, spatially isolating reactive groups until triggering. Overall, this work translates the amplification of HCR into small molecule release without the use of multiple components, and will aid its application to biosensing, imaging and drug delivery.

Introduction

Concealing the activity of functional small molecules, such as fluorescent or therapeutic structures, and triggering their release in active form in response to a biological stimulus has important applications in a variety of different areas including smart therapeutics, biological detection and bio-imaging.[1] Nucleic acids are favorable biological molecules to trigger the release of pro-functional small molecules, because of their protein recognition properties (e.g., aptamers) and unique spatiotemporal expression profiles (e.g., mRNA, miRNA). They have thus been used as both triggers and recognition components in a variety of stimuli-responsive nanodevices.[2] However, many of these devices respond to a stoichiometric amount of stimulus, and thus, the typically small amounts of biological targets present *in vitro* or *in vivo* would not be sufficient to elicit a sizable response.[3]

To address this issue, many amplification methods have been developed.[4] Notably, the release of functional small molecules via nucleic acid-templated catalysis has emerged as a powerful tool to amplify nucleic acid signals into detection and drug release responses.[4c, 5] This approach uses two DNA-small molecule conjugates, which perform a DNA-templated reaction with each other upon binding a nucleic acid target. The reaction releases the small molecule payload from the conjugate, allowing it to elicit its function.[5b] While this is a powerful method, it does require separate components that are able to reversibly bind the target template in order to generate turnover, making it primarily feasible *in vitro*.[6] Due to differences in pharmacokinetics and tissue distribution of different components, it would be desirable to combine the amplification system into a single nanodevice for *in vivo* applications.

Integrating reactive functional groups into a single device, however, poses the significant challenge of preventing the groups from reacting non-specifically until they are triggered. Some natural systems have evolved unique mechanisms to spatially isolate different reactive groups within the same structure.[7] Enzymes such as plasminogen[8] and vascular endothelial growth factors C & D[9], have precisely placed intramolecular reactive thiol and disulfide moieties, which are brought in close proximity upon allosteric recognition. In DNA nanotechnology, reactive functional groups can be effectively separated for sequential transfer reactions in the form of a DNA walker.[10]

In addition to DNA-templated chemical reactions, amplification methods that rely on toehold mediated strand displacement have been extensively investigated.[11] For example, enzyme-free isothermal amplification methods, such as the hybridization chain reaction (HCR)[4a, 12] or catalytic hairpin assembly (CHA)[4b] rely on metastable hairpins for amplification. Furthermore, the different component molecules necessary for these methods have been combined into single metastable nanodevices using DNA nanotechnology approaches.[13] HCR in particular has been used for bio-sensing assays[14], bio-imaging[15], bio-medicine[16], and small molecule synthesis[17]. While previous HCR-small molecule hybrids have been generated that release through non-specific hydrolysis[16b] or diffusion[16a, 18], to our knowledge HCR has not been developed for the conditional release of small molecules.

Here, we set out to develop the hybridization chain reaction for the conditional, amplified release of pro-functional small molecules. Combining HCR with a DNA-templated reaction and strategically positioning reactive functional groups on each hairpin allows these reactive groups to be kept separated under high dilution conditions. Once polymerization is induced, the reactive groups increase in effective concentration and are able to trigger a self-immolative mechanism, releasing functional small molecules in an amplified manner.

Importantly, this method operates using toehold-mediated strand displacement with metastable hairpins, allowing their combination into complex structures. By using different DNA nanostructures, such as polymerizable tracks and spherical nucleic acids, we show that both HCR hairpin components can be integrated into a single structure, while effectively separating reactivity until triggering. Using DNA nanotechnology allows for the organization of different functional components with high precision and structural control.

In this contribution, HCR is the tool used to achieve amplification, but the innovation in our approach lies in the spatial separation of chemically reactive functional groups within the same nanostructure, for triggered amplified release of small molecules. This required careful synthetic and kinetic studies, which will be valuable for the diagnostic and therapeutic communities. We anticipate that the development of these systems can lead to new analytical tools for biosensing and

[*] A. L. Prinzen, D. Saliba, C. Hennecker, T. Trinh, Prof. A. Mittermaier, Prof. H. F. Sleiman
Department of Chemistry, McGill Univerisity
801 rue Sherbrooke West, Montreal, QC, H3A 0B8 (Canada)
E-mail: hanadi.sleiman@mcgill.ca

Supporting information for this article is given via a link at the end of the document.

10.1002/anie.202001123

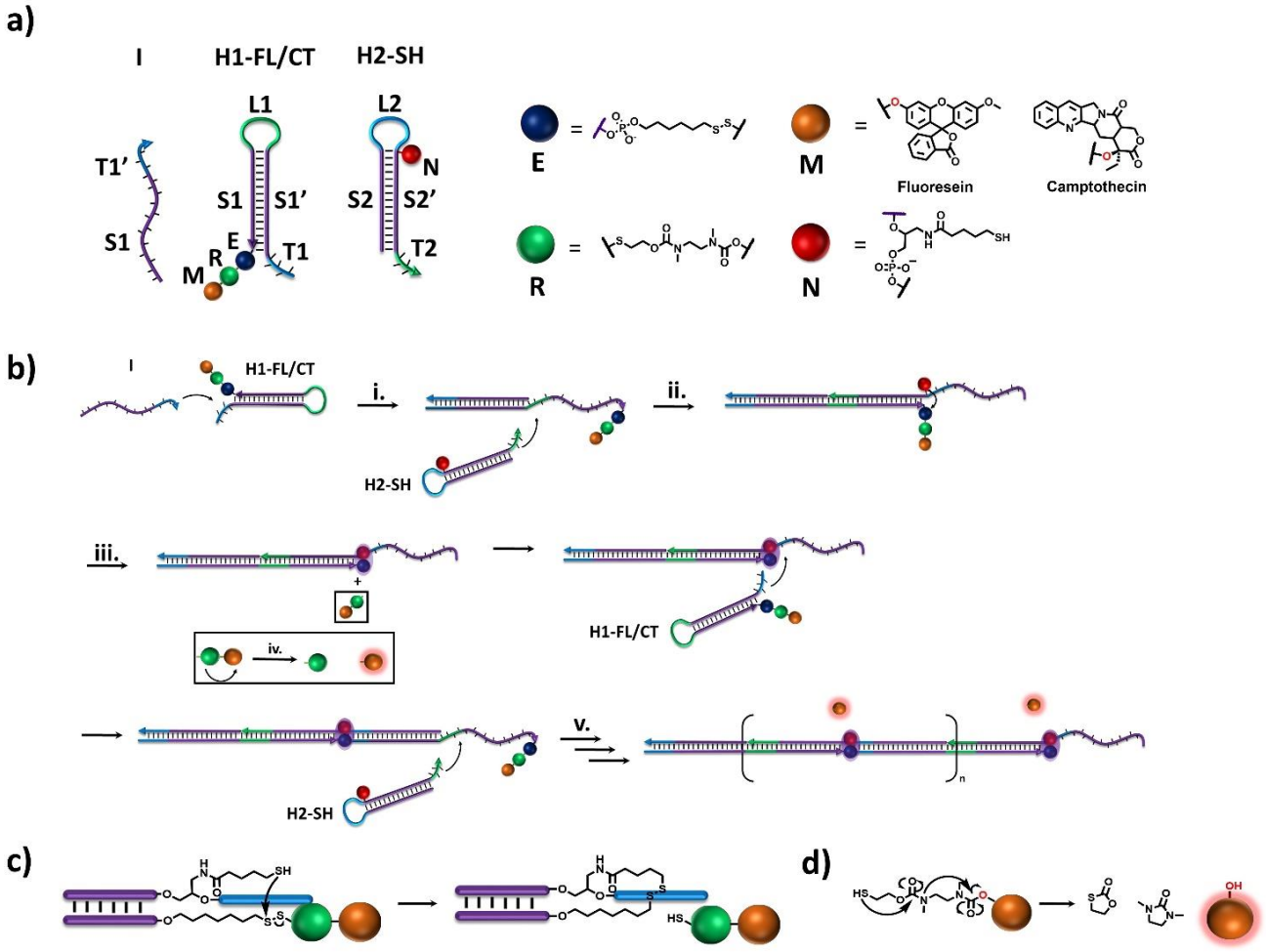

Figure 1. (a) Design of H1-Fl/ H1-CT and H2-SH for HCR (b) Mechanism of HCR resulting in the release of pro-functional molecules: i. initiator hybridizes to the toehold domain of H1 and performs a toehold mediated strand displacement. ii. Loop domain of H1 hybridizes to the toehold domain of H2 and performs a toehold mediated strand displacement. iii. DNA templated reaction occurs, releasing the pro-functional molecule connected to a biodegradable linker. iv. Immolative linker degrades to release the functional molecule in its active form. v. The HCR process repeats polymerizing H1 and H2, amplifying the release of pro-functional molecule. (c) Mechanism of DNA templated disulfide exchange, resulting in the release of the pro-functional molecule. (d) Mechanism of immolative linker degradation, resulting in the release of active molecule.

bioimaging as well as stimuli-responsive drug delivery vehicles. Our approach is a combination of two areas of research: DNA-templated catalysis and DNA-based amplification methods like HCR. In principle, it can be applied to any DNA based toehold mediated amplification methods such as CHA.[4b]

Results and Discussion

Design, Synthesis and Characterization of HCR. In order to use HCR for conditional release, two processes are required, 1) HCR polymerization for amplification and 2) a DNA mediated bond cleavage reaction that occurs after polymerization to liberate the small molecules.

In the simplest version of HCR there are two hairpins (H1 & H2) that are designed to have a toehold domain (T), a stem domain (S) and a loop domain (L). Both the toehold and loop domains on opposite hairpins are complementary to each other, but are kinetically trapped and do not hybridize (Figure 1a.). The HCR process begins when an initiator strand (I) is introduced, binding to the toehold domain of H1, displacing the stem domain, and revealing the loop domain (Figure 1b-i). From here the loop domain of H1 binds to the toehold domain of H2, displacing its stem domain and revealing its loop domain (Figure 1b-ii). This process repeats until all of H1 and H2 are consumed, generating amplification with long polymers of H1 and H2 (Figure 1b-v).

To address the second process, each of the hairpins in the HCR process was modified with unique design features. To the stem domain of H1 was added a reactive group (E), connected through a linker group (R) to the small functional molecule (M) (Figure 1a.). H2 was modified between the stem and loop domains with another reactive group (N). The groups (E) and (N) serve the purpose of reacting together in a bond cleavage process. After polymerization these groups would be strategically placed in close proximity on each monomer to increase their effective concentration and react as a DNA templated reaction (Figure 1b-iii). We chose to use a DNA-templated sulfide nucleophilic attack for the bond cleavage reaction (Figure 1b). DNA-templated thiol-disulfide exchange has typically been used as a DNA ligation reaction[19], but also in nucleic acid templated catalysis[20]. In our design, the (E) domain of H1 is a disulfide that can be cleaved by the thiol group (N) of H2, releasing the (R) and (M) groups. Interestingly, this DNA-templated reaction is accompanied by covalent bond formation between (E) and (N) in the resulting polymer (Figure 1c). To our knowledge this would be the first time that HCR is accompanied by component ligation. In addition to providing an additional method to monitor the process using

denaturing gel electrophoresis (see below), this results in a more stable, less dynamic polymer which makes it a useful material, rather than only a side-product.

In addition to the bond cleavage reaction, we also required a method to conceal and then recover the activity of the small molecule (M). Therefore, we introduced a self immolative linker (R) between (E) and (M). Using the self-immolative linker (R) gives us a traceless degradable linker that is triggered by the bond cleavage reaction (Figure 1b iv). More specifically, while (M) and (R) are connected to (E) its activity is sequestered until the DNA templated bond cleavage reaction occurs and the self immolative linker undergoes a series of intramolecular cyclizations to release the small molecule (M), recovering its activity (Figure 1d). We introduced an extra diethylamine linkage into (R) to form carbamate linkages, as opposed to carbonate linkages, as this had been shown previously to reduce non-specific hydrolysis of the functional molecule from the linker.[21] To monitor the extent and rate of small molecule release in real time by fluorescence spectroscopy we initially chose (M) to be a methoxyfluorescein molecule (Figure S1), that is non-emissive when connected to the self immolative linker.[22]

Modified H1 and H2 strands were synthesized, and reacted to generate methoxyfluorescein conjugated H1 (H1-FL) and thiol modified H2 (H2-SH). These strands were then characterized by gel electrophoresis and LC/MS (Detailed synthesis and characterization SI-VI.). For H2-SH, it was non-trivial to install an internal thiol modification, as complex synthesis and purification factors must be considered and there are limited commercial reagents available (Detailed in SI-VI.). Briefly, to overcome these challenges we functionalized H2 with a serinol amino modification in the desired location and labelled it on the solid support with an activated ester molecule containing a disulfide, before the final deprotection. Stability of the H1-FL strand was confirmed by fluorescence and high performance liquid chromatography (HPLC), with no appreciable degradation over 24 hrs (Table S3 and Figure S14).

We are able to monitor the system using three methods 1) the degree of monomer consumption, as determined by native agarose gel electrophoresis gel electrophoresis (AGE), which informs on the efficiency and rate of the HCR process (Figure 2a and Figure 2c) 2) the degree of ligation as determined by denaturing AGE, which informs on the yield and kinetics of release of the pro-methoxyfluorescein molecule (Figure 2b and Figure 2c) and 3) fluorescence intensity increase of the fluorophore, which informs on the yield and rate of the self-immolative cyclization's to produce the active molecule (Figure 2c). First, to determine the extent of amplification, we performed our polymerizations at a constant hairpin concentration of 750nM, while varying the amount of initiator between 0 and 1 equiv. (Table S3, Figure S12 and Figure S14).

It was found that between 1 and 0.1 equiv. of initiator, our system polymerized to ≈90% (Figure 2a). At 0.1 equiv. of initiator the polymerization afforded approx. 640 nM of released methoxyfluorescein which is significantly more than the concentration of initiator (75 nM), indicating amplified release (Figure 2c and Figure S14). This represents an 85% yield over three steps (Polymerization, ligation & linker degradation) with respect to the concentration of H1-FL (Figure 2c). Even at 25nM initiator concentration we were able to release 340 nM of methoxyfluorescein which approaches the concentration of some relevant biomarkers (Figure S14).[23] The ligation product of H1-FL and H2-SH was further confirmed by LC-MS (Figure S15). We confirmed that the disulfide exchange reaction was still viable over time and that the overall yield was not reduced due to non-specific thiol oxidation by performing a series of polymerizations initiated at different time points (Figure S16).

For the sequences used, circuit leakage at 0 equiv. of initiator was found to be only 5% after 1hr up to a maximum of approx. 20% over 24hrs (Figure 2c and Figure S14). We determined that circuit leakage was not due to non-specific reactions between H1-FL and H2-SH by exposing H1-FL to a non-hybridizing H2-SH (H2-2-SH), resulting in minimal release (Figure S12 and Figure S14). Therefore, it was determined that leakage is primarily due to spontaneous polymerization between H1-FL and H2-SH when no initiator is present. Leakage was further reduced to <10% over 24hr in the second generation by increasing the stem length of the hairpins from 12 to 18 bases, (see below).

In order to verify that our system follows the intended HCR mechanism (Figure 1b), the kinetics of assembly were analyzed according to the scheme shown in Figure 2e. The initiator, I, and polymer $I(H1H2)_n$ bind to hairpin H1, and the IH1 dimer and polymer $I(H1H2)_nH1$ bind to H2 according to the second-order rate constant k_1. These steps were assumed to have identical kinetics, since the toe-hold and stem loop regions are identical in H1 and H2. The ligation of adjacent H1 and H2 fragments (and concomitant release of the pro-functional molecule) obeyed first-order kinetics with rate constant k_2. The immolative cyclization reaction was described with the first-order rate constant k_3. Theoretical kinetic traces were obtained by numerically integrating the coupled differential equations (see Supporting Information). The native AGE, denaturing AGE, and fluorescence data were fit to this kinetic scheme by non-linear least squares minimization, yielding the rate constants k_1, k_2, and k_3. In addition, we found it necessary to account for a small amount of unreacted material present at the end of the reactions, which can be attributed to misfolded secondary structures, spurious synthesis errors, and/or stoichiometric concentration differences between the two DNA strands (Figure 2a).[24] We therefore included an adjustable parameter in the fits describing the concentration of inactive or "misfolded" H1 and H2 strands and assumed equal quantities of both.

Kinetics were assessed at 0.1eq of initiator at 25°C, and the calculated curves were in excellent agreement with the experimental data, giving us a high degree of confidence that this system follows an HCR mechanism (Figure 2d). The total amount of misfolded material was found to be 144 ± 5 nM, reducing the effective starting concentration of each hairpin from 750 nM to about 606 nM. The association rate constant (k_1) was found to be $1{\cdot}10^4 \pm 1{\cdot}10^3$ M^{-1} s^{-1}. This is slightly slower than reported in previous studies of hairpin-hairpin interactions, possibly due to the additional functional groups present in the H1-FL and H2-SH strands (Figure 2d and Figure S17).[25] We found that the ligation step was much faster than H1/H2 association, meaning that the rate of pro-functional molecule release is governed almost exclusively by k_1. It was therefore not possible to extract a precise value for k_2, though a lower bound of $\gtrsim 1{\cdot}10^{-3}$ s^{-1} was obtained. Finally, the rate of the immolative cyclisation's (k_3) was found to be $2.1{\cdot}10^{-4} \pm 3{\cdot}10^{-5}$ s^{-1}, making it the slowest step of the reaction. It is likely also the slowest step in templated HCR, as templation can accelerate HCR by two orders of magnitude.[13d]

To showcase the versatility of our system to release different functional molecules we generated another H1 hairpin making (M) a camptothecin prodrug (H1-CT) (Figure S2 for detailed synthesis and structure). The amount of release from H1-CT, was monitored through native/denaturing agarose and HPLC analysis. Release was found to be comparable the H1-FL releasing 80-95% of the camptothecin prodrug (Figure S18 and Table S6).

Looking towards future applications of our system, we analysed the release of small molecule from H1-FL in response to biologically relevant reducing conditions. We exposed H1-FL to both extracellular (0.01mM) and intracellular (1mM), levels of free thiols, in the form of DTT.[26] Release was monitored by fluorescence and HPLC analysis. Minimal release was found when H1-FL was exposed to extracellular levels of reducing agent over 24hrs, while intracellular levels of reducing agent cleaved the small molecule from H1-FL (Figure S19 and Table S7). Given the wealth of HCR sequences which respond to various extracellular signals through the use of aptamers, we anticipate that our system could operate through extracellular recognition and release events followed by drug internalization.[16b, 27] This may be

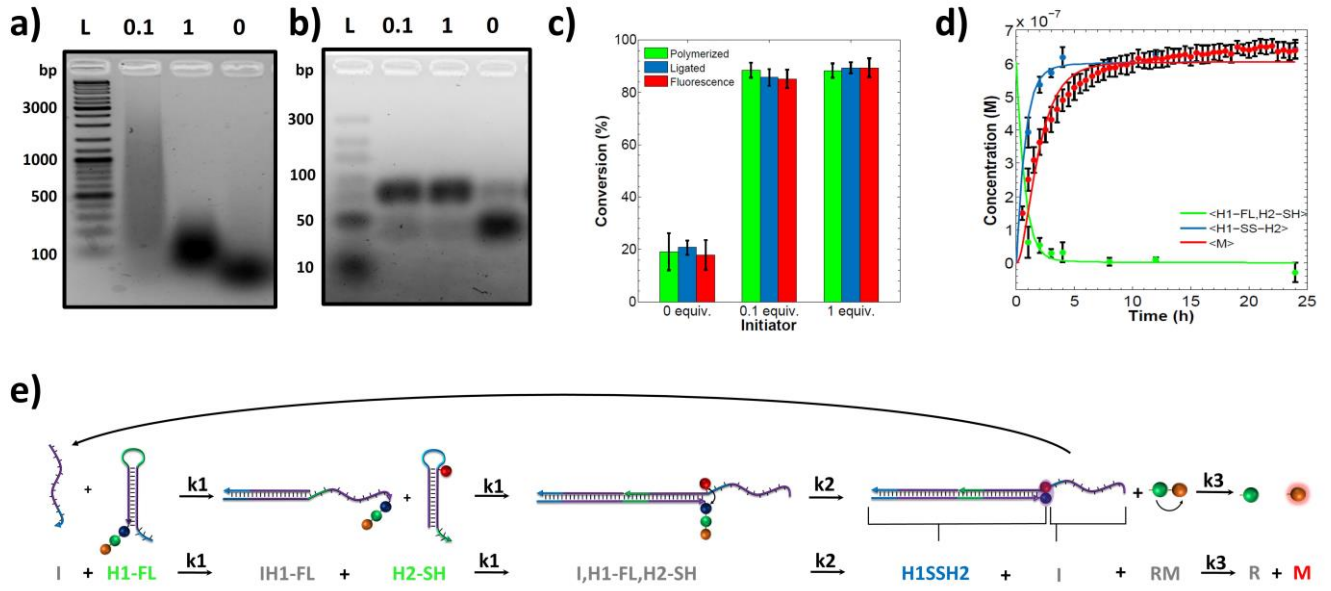

Figure 2. Characterization of HCR between H1-FL and H2-SH after 24hr, by (a) Native agarose and (b) Denaturing agarose: L: Ladder, Lane 0: H1-FL + H2-SH, Lane 0.1: Lane 0 + 0.1 equiv. I-1, Lane 1: Lane 0 + 1 equiv. I-1. d. (c) Degree of monomer consumption, ligation and released methoxyfluorescein after 24 hr, of H1-FL and H2-SH with 0, 0.1 and 1 equiv. I-1. (d) HCR kinetics, experimental data is represented as circles and simulated kinetics are solid lines. Error bars correspond to the standard deviation of triplicate measurements. Native-AGE (green) is reported as the average value of H1 and H2 strands, denatured-AGE (blue) is reporting on ligated H1H2 complexes, fluorescence measurements (red) report on the completion of immolative cyclization. (e) Sequential mechanism of the HCR reaction with ligation and immolative cyclization steps, the colours of each species correspond to their traces in d, species that were not measured are represented in grey (see SI-VIII. Figure S17 for more detail.).

a more viable method without the need to internalize the DNA component which is always a challenge for oligonucleotide therapeutics.[28]

Design, Synthesis and Characterization of DNA Templated HCR. Having shown that we could indeed amplify the release of functional molecules using HCR, we then investigated whether both components could be integrated into a single nanodevice. Localized HCR has been recently shown to accelerate the rate of HCR on single stranded and DNA origami templates.[13c, 13d] This strategy operates by anchoring the hairpins to a single scaffold, increasing their effective concentration. A major advantage of anchoring the hairpins is that a robust nanostructure is formed which is more desired for *in vivo* applications. However, the hairpins of the circuit in this previous strategy are all unique in sequence and required to be precisely placed on the scaffolds, hindering scalability. Additionally, the extent of polymerization was controlled by the size of the scaffold, and while this may be beneficial for creating defined circuits, limits amplification to the size of the scaffold. Another recent strategy to localize HCR has been to selectively recruit the HCR hairpins with a supramolecular scaffold, using a short reversible hybridization region.[29] In this case, the hairpins no longer needed to be precisely placed and the extent of polymerization was no longer confined to the template, however, this results in a weakly held construct that is more suited to *in vitro* than *in vivo* applications

Keeping these two strategies in mind, we developed a design that allows us to generate a robust structure with two hairpins anchored to a short DNA scaffold. This results in a two-hairpin monomer that can polymerize upon analyte recognition (Figure 3a). Using a design like this means that 1) HCR is not limited to the size of the scaffold, and 2) only two hairpins need to be precisely placed. To achieve this, our design makes some changes to the sequences of the original HCR system.

First, to avoid circuit leakage, we increased the stem length (S) of the hairpins from a 12 to an 18 b.p. hybridization region. Next we extended the 5' and 3' ends of the H1 and H2 hairpins in order to provide a hybridization region (A) that could then be used to hybridize to a DNA scaffold (B') via adapter strands S1 & S2 with sequence (A-B) (Figure 3a.). Sequence's B1 and B2 were designed to be two turns of DNA, orienting the hairpins on the scaffold in the same direction. Additionally, we added a spacer region (X) next to the loop region (L) of the hairpins as this had been shown previously to allow templated HCR to occur without steric constraints.[13c] We calculated that, for our system, adding 11 T spacers was sufficient to allow the loop region of one hairpin unit to hybridize with the overhang region of the next hairpin unit, once initiated (Figure 3a).

Polymerization of the single unit occurs by an intermolecular initiation of H1 (Figure 3d-i) on the template followed by an intramolecular hybridization to H2 (Figure 3d-ii). Here, a nucleic acid templated reaction can occur, releasing the cargo (Figure 3d-iii). Additionally, H2 is available for an intermolecular hybridization to H1 on another unit, the whole process then repeats growing the polymer (Figure 3d-v and Figure 3d-vi).

For this design two types of DNA templates were generated for HCR, one with blunt ends on the template (BBB) and the other with short sticky ends (SBB) (Figure 3b). Inspired by the supramolecular scaffold method of localized HCR, we hypothesized that the short sticky ends could improve propagation of the HCR unit, by reversibly associating the individual units together, giving overall enhanced kinetics for release.

The modified hairpins were synthesized using the general procedure to generate H1-2-FL and H2-2-SH (Detailed in SI-VI.). Before moving forward with the templated HCR, we first examined the effect of the changes made to H1-FL and H2-SH had on leakage and polymerization without using a template (NT). By increasing the stem (S) of these hairpins from 12 to 18 bps, the resulting leakage was ≤10% over 24hrs. Next, we introduced the hairpins to 1 equiv. (750nM) of initiator strand (I-2) and found that over 24 hrs, approximately 560 nM of the conjugate was released, representing a 75% yield over 3 steps. With 0.1 equiv. of initiator (75 nM) approximately 490 nM of the conjugate was released, indicating that amplification was once again achieved, and

10.1002/anie.202001123

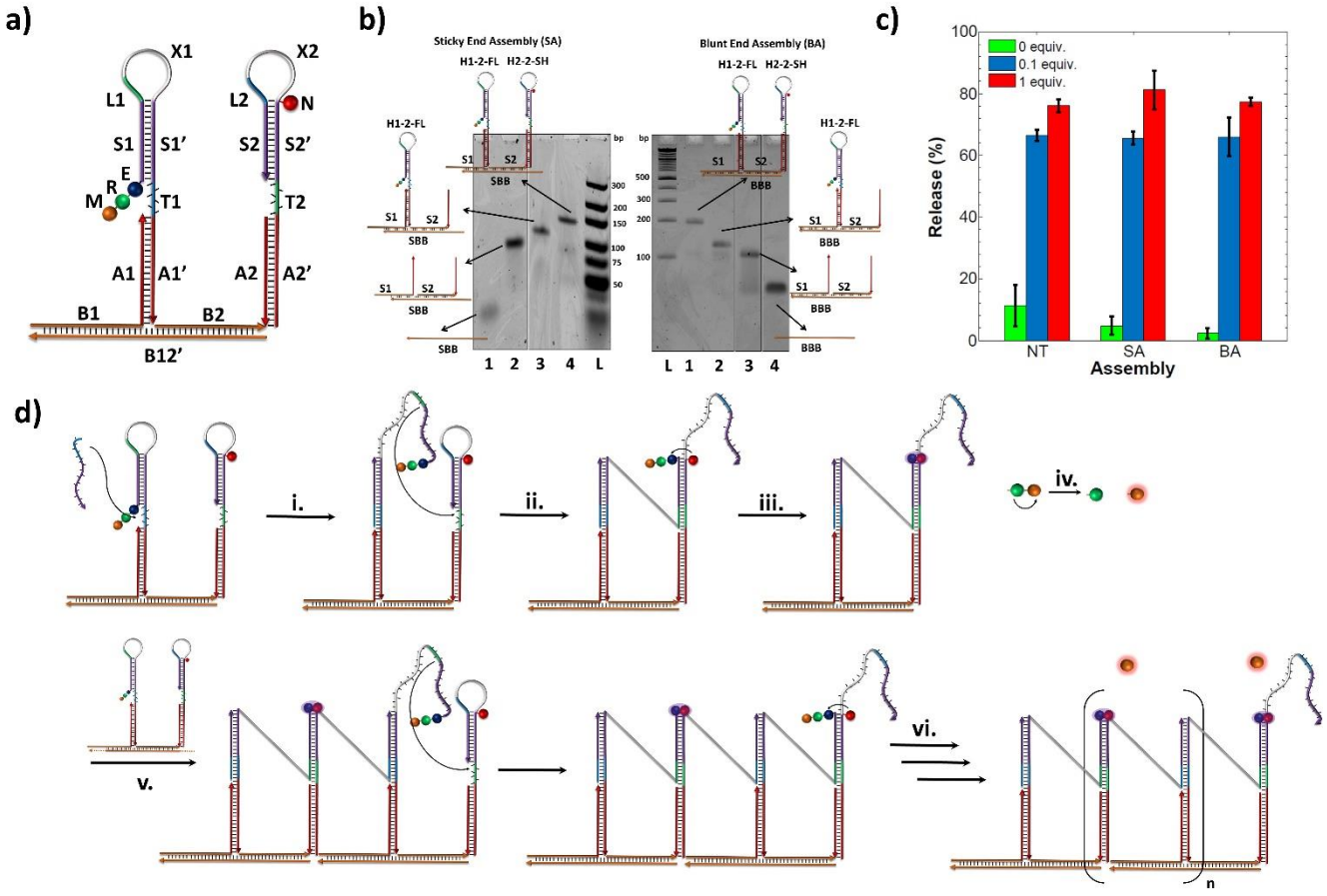

Figure 3. (a) Design of Blunt (BA) end assembly with H1-2-FL and H2-2-SH hairpins. (b) Native PAGE of the assembly of BA and SA. (c) Release of methoxyfluorescein from the HCR of H1-2-FL and H2-2-SH with 0, 0.1, and 1 equiv. of I-2, on No Template (NT), SA, and BA after 24hr, fluorescence was measured at λ_{ex}= 470 nm, λ_{em}= 515 nm. (d) Mechanism of HCR by the BA: i. Initiator hybridizes intermolecularly to T1 of H1-2-FL and performs a strand displacement, exposing the L1 region. ii. L1 hybridizes intramolecularly to T2 on H2-2-SH and performs a strand displacement to expose the L2 region. iii. a DNA templated reaction occurs releasing the pro-functional molecule connected to the immolative linker. iv. Degradation of the immolative linker to release the active functional molecule. v. L2 region hybridizes intermolecularly to the T1 region of another BA unit. vi. Polymerization continues, amplifying the release of active molecule.

representing a 65% yield over 3 steps (Figure 3c). Analysis of the native agarose gel reveals that the polymerized species seem to have lower average molecular weight distributions (Figure S20a, lane NT-0.1), than the original counterparts (Figure S12a. lane 5). We suspect that with the changes made to the hairpins, the propagation rate of polymerization has been slowed down (H1 hybridizing to H2), while the initiator binding step is still rapid (I hybridizing to H1).

Confirming that HCR still works with these changes, we then moved on to generate the sticky (SA) and blunt (BA) ended assemblies. To make the assemblies we pre-annealed each of the hairpins separately for correct folding, and then hybridized them with each template at room temperature (Figure 3b, detailed in SI-IX). Control experiments without initiator showed the absence of non-specific reactivity between the H1-2-FL disulfide and the H2-2-SH thiol, as leakage was comparable to the non-templated hairpins (Figure 3c and Figure S20-S22). Upon adding 1 equiv. and 0.1 equiv. of initiator strand (I-2) to each of the assemblies, we found that the yields and amplification were maintained compared to the non-templated hairpins, 75% and 65% respectively, amplifying approximately 6.5x (Figure 3c).

Comparing the sticky and blunt ended assemblies when 1 equiv. of initiator is added (Figure S20, lanes SA-1 & BA-1), the blunt ended assemblies remain more defined and do not appear to polymerize as the sticky ended assemblies. We hypothesize that this is due to a combination of slow propagation and a pre-organization effect with the sticky ended assemblies. If, in solution the sticky ended assemblies are pre-organized, then when initiator is introduced instead of polymerizing uni-directionally, the polymerization can occur in two directions (Figure S24). Statistically this can leave un-hybridized hairpins in the middle of the pre-organized polymer, which then can only hybridize intermolecularly. Indeed, when we look at the atomic force microscopy (AFM) of the sticky, and blunt ended assemblies and no template with 0.1equiv of initiator we find that there is more bundling of the sticky ended assemblies, than the blunt ended assemblies and no template, indicating increased intermolecular branching between units (Figure S23).

Ultimately, we found that the rate of release between the sticky and blunt ended assemblies and no template remained unchanged (Figure S22). This is consistent with remaining intermolecular hybridizations between units, and the slowest step being the immolative cyclization's to activate the fluorophore. Based on the native gel and AFM analysis we can infer that the intramolecular hybridizations do in fact occur faster than intermolecular hybridizations, however more detailed studies on strictly the rate of polymerization would be needed to confirm. Overall, it was successfully established that we could in fact integrate a set of reactive hairpins into a single nanodevice, and selectively activate the amplified release of pro-functional small molecules in response to a DNA signal. Interestingly, the HCR process also results in a cross-linked and rigid polymeric

10.1002/anie.202001123

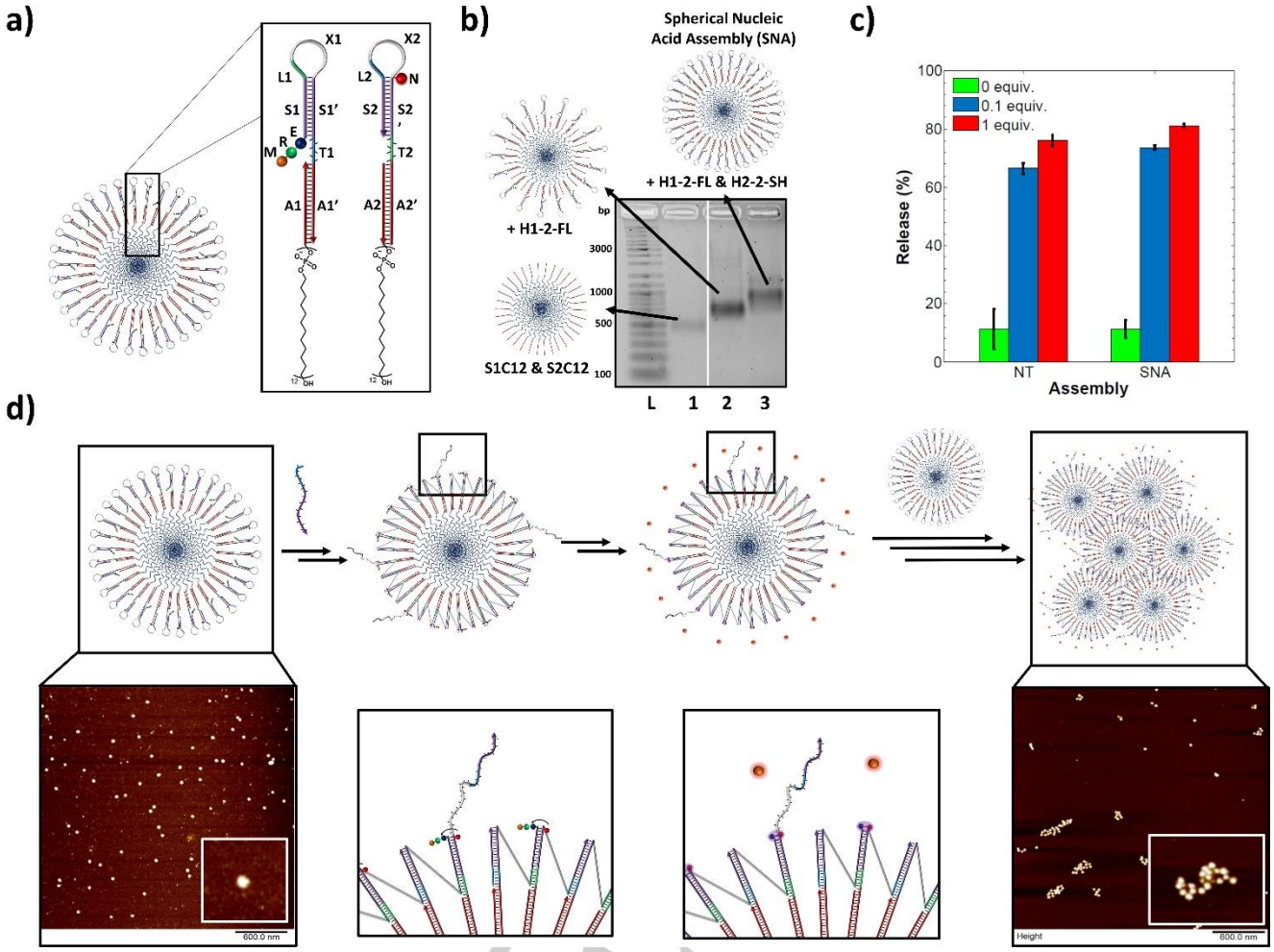

Figure 4. (a) Design of Spherical nucleic acid (SNA) assemblies for HCR between H1-2-FL and H2-2-SH. (b) Native agarose of the SNA assembly. (c) Release of methoxyfluorescein from the HCR of H1-2-FL and H2-2-SH with 0, 0.1, and 1 equiv. of I-2, on No Template (NT) and SNA assembly after 24hr, fluorescence was measured at λ_{ex}= 470 nm, λ_{em}= 515 nm. (d) Mechanism and AFM characterization of the release of functional molecules from the SNA assembly, resulting in clustering of the SNA's.

nanostructure that is partially ligated, and the presence of this structure at e.g., the disease site could possibly contribute a therapeutic effect. This approach would be similar to enzyme-triggered peptide self-assembly, which has been shown to selectively kill cancer cells.[30]

Design, Synthesis and Characterization of Spherical Nucleic acid Templated HCR. Having shown the integration of a pair of hairpins into a single device, we next wanted to investigate integrating multiple hairpins into a single nanodevice. Spherical nucleic acids have been extensively studied for their cellular uptake and nuclease resistance properties and provide us a 3D platform for templation of the HCR reaction.[31]

In our lab we have developed sequence controlled spherical nucleic acids that are made through the introduction of dodecane phosphoramidites, providing a hydrophobic block for self-assembly.[32] For our purposes here, we generated two amphiphilic nucleic acids with opposite directionalities using this method. Each of these strands is then able to hybridize to the overhang region (A) on the previously generated H1-2-FL and H2-2-SH hairpins, giving them the correct directionality for the HCR process to occur (Figure 4a). The assemblies were generated in a stepwise fashion by first generating the spherical nucleic acid and sequentially adding each hairpin (Figure 4b, detailed in SI-X.). After the assemblies were generated, we found that there was minimal leakage (≤10%) of the system over 24hrs by HPLC, native/denaturing & fluorescence (Figure 4c. and Figure S25-S27).

The amount of release was then monitored in response to 1 and 0.1equiv of initiator (I-2). Here we found that the yields were slightly improved from 75% to 82% for the 1equiv and from 66% to 74% for 0.1equiv of initiator, over three steps (Figure 4c.). Once again we were able to amplify the signal of 75 nM by releasing 560 nM of methoxyfluorescein, giving us an overall amplification of approximately 7.5x. Additionally, we characterized the HCR polymerization by dynamic light scattering (DLS) and atomic force microscopy (AFM). By both of these techniques we observed that the particles clustered together when 1 or 0.1 equiv. of initiator strand was added, generating large aggregates of SNA's (Figure 4d and Figure S28). These changes in morphology in response to a low amount of DNA signal may be of further interest for future dynamic nanotechnology studies. In contrast to the approach in Fig. 3, the SNA carries multiple hairpins, rather than just two, and each SNA nanostructure can release a relatively large number of small molecules. Using spherical nucleic acids as the platform for HCR allows for localization of multiple HCR components in a single device and is more suited for future *in vivo* studies, where distribution of different components may differ.

Conclusion

In this work we first demonstrate that by rationally placing disulfide and thiol functionalities on opposite hairpins of HCR we can amplify a DNA signal to selectively release small molecules. This is the first time HCR has been used for the triggered release of small molecules which can be monitored in three ways 1) by the degree of monomer consumption, 2) by the degree of ligation and 3) by fluorescence intensity. Unlike previous HCR methods where small molecule cleavage is non-specific, our construct is built to only carry out reactions in the presence of an initiator, significantly decreasing non-specific cargo release. Our synthetic approach can also be applied to other DNA toehold-mediated amplification processes, such as CHA. Additionally, we were able to take advantage of the metastability of the HCR hairpins and integrate both reactive hairpins into single unit nanodevices. We used both DNA and SNA assemblies which, importantly, were able to separate reactive functional groups and isolate reactivity, preventing release, and amplify release when triggered. The nanostructures not only release small molecules, but in addition conditionally generate a partially ligated, crosslinked DNA polymer, which could have added therapeutic effects, in analogy to enzyme-driven peptide assembly. Given the abundance of DNA templated reactions and different HCR sequences, future work will focus on increasing sensitivity and accelerating the kinetics, and adapting this method for *in vitro/vivo* release applications.

.

Acknowledgements

This work was supported by NSERC, FRQNT, CFI, and the Canada Research Chairs Program. A.P. thanks NSERC for a graduate scholarship. H.F.S thanks the Canada Council for the Arts for a Killam Fellowship. H.F.S is a Cottrell Scholar of the Research Corporation. H.F.S. and A.P. also thank the Mass Spectroscopy Facility (McGill University) for their help with the HPLC, and LC-MS experiments.

Keywords: Dynamic DNA Nanotechnology • Isothermal Amplification • Self-Immolative • Nucleic Acid Templated Catalysis

[1] M. Di Pisa, O. Seitz, *ChemMedChem* **2017**, *12*, 872-882.
[2] a) D. M. Kolpashchikov, *Acc. Chem. Res.* **2019**, *52*, 1949-1956; b) Y. Yu, B. Jin, Y. Li, Z. Deng, *Chemistry – A European Journal* **2019**, *25*, 9785-9798.
[3] a) H. H. Fakih, J. J. Fakhoury, D. Bousmail, H. F. Sleiman, *ACS Appl. Mater. Interfaces* **2019**, *11*, 13912-13920; b) K. E. Bujold, J. C. C. Hsu, H. F. Sleiman, *J. Am. Chem. Soc.* **2016**, *138*, 14030-14038; c) F. Nagatsugi, S. Nakayama, S. Sasaki, *Nucleosides, Nucleotides Nucleic Acids* **2007**, *26*, 799-803; d) A. Okamoto, K. Tanabe, T. Inasaki, I. Saito, *Angew. Chem. Int. Ed.* **2003**, *42*, 2502-2504; e) K. E. Bujold, J. Fakhoury, T. G. W. Edwardson, K. M. M. Carneiro, J. N. Briard, A. G. Godin, L. Amrein, G. D. Hamblin, L. C. Panasci, P. W. Wiseman, H. F. Sleiman, *Chemical Science* **2014**, *5*, 2449-2455.
[4] a) R. M. Dirks, N. A. Pierce, *Proc. Natl. Acad. Sci. U. S. A.* **2004**, *101*, 15275-15278; b) P. Yin, H. M. T. Choi, C. R. Calvert, N. A. Pierce, *Nature* **2008**, *451*, 318; c) Z. Ma, J. S. Taylor, *Proc. Natl. Acad. Sci. U. S. A.* **2000**, *97*, 11159-11163.
[5] a) K. Gorska, A. Manicardi, S. Barluenga, N. Winssinger, *Chem. Commun.* **2011**, *47*, 4364-4366; b) Z. Ma, J.-S. Taylor, *Bioorg. Med. Chem.* **2001**, *9*, 2501-2510; c) D. Chang, E. Lindberg, N. Winssinger, *J. Am. Chem. Soc.* **2017**, *139*, 1444-1447; d) K. K. Sadhu, N. Winssinger, *Chemistry – A European Journal* **2013**, *19*, 8182-8189; e) H. Wu, S. C. Alexander, S. Jin, N. K. Devaraj, *J. Am. Chem. Soc.* **2016**, *138*, 11429-11432; f) K. T. Kim, S. Angerani, D. Chang, N. Winssinger, *J. Am. Chem. Soc.* **2019**, *141*, 16288-16295.
[6] L. Holtzer, I. Oleinich, M. Anzola, E. Lindberg, K. K. Sadhu, M. Gonzalez-Gaitan, N. Winssinger, *ACS Central Science* **2016**, *2*, 394-400.
[7] J. Chiu, P. J. Hogg, *The Journal of biological chemistry* **2019**, *294*, 2949-2960.
[8] D. Butera, T. Wind, A. J. Lay, J. Beck, F. J. Castellino, P. J. Hogg, *The Journal of biological chemistry* **2014**, *289*, 2992-3000.
[9] J. Chiu, J. W. H. Wong, M. Gerometta, P. J. Hogg, *Biochemistry* **2014**, *53*, 7-9.
[10] Y. He, D. R. Liu, *Nat. Nanotechnol.* **2010**, *5*, 778.
[11] D. Y. Zhang, G. Seelig, *Nature Chem.* **2011**, *3*, 103-113.
[12] H. M. T. Choi, V. A. Beck, N. A. Pierce, *ACS Nano* **2014**, *8*, 4284-4294.
[13] a) K. Ren, Y. Xu, Y. Liu, M. Yang, H. Ju, *ACS Nano* **2018**, *12*, 263-271; b) G. Chatterjee, N. Dalchau, R. A. Muscat, A. Phillips, G. Seelig, *Nat. Nanotechnol.* **2017**, *12*, 920; c) H. Bui, V. Miao, S. Garg, R. Mokhtar, T. Song, J. Reif, *Small* **2017**, *13*, 1602983; d) H. Bui, S. Shah, R. Mokhtar, T. Song, S. Garg, J. Reif, *ACS Nano* **2018**, *12*, 1146-1155; e) J. Wang, D.-X. Wang, J.-Y. Ma, Y.-X. Wang, D.-M. Kong, *Chemical Science* **2019**.
[14] C. R. Park, S. J. Park, W. G. Lee, B. H. Hwang, *Biotechnol. Bioprocess Eng.* **2018**, *23*, 355-370.
[15] H. M. T. Choi, J. Y. Chang, L. A. Trinh, J. E. Padilla, S. E. Fraser, N. A. Pierce, *Nat. Biotechnol.* **2010**, *28*, 1208-1212.
[16] a) G. Zhu, J. Zheng, E. Song, M. Donovan, K. Zhang, C. Liu, W. Tan, *Proceedings of the National Academy of Sciences* **2013**, *110*, 7998-8003; b) Y.-M. Wang, Z. Wu, S.-J. Liu, X. Chu, *Anal. Chem.* **2015**, *87*, 6470-6474.
[17] W. Meng, R. A. Muscat, M. L. McKee, P. J. Milnes, A. H. El-Sagheer, J. Bath, B. G. Davis, T. Brown, R. K. O'Reilly, A. J. Turberfield, *Nature Chem.* **2016**, *8*, 542.
[18] T. Jiang, L. Zhou, H. Liu, P. Zhang, G. Liu, P. Gong, C. Li, W. Tan, J. Chen, L. Cai, *Anal. Chem.* **2019**, *91*, 6996-7000.
[19] a) M. De Stefano, K. Vesterager Gothelf, *ChemBioChem* **2016**, *17*, 1122-1126; b) M. L. McKee, A. C. Evans, S. R. Gerrard, R. K. O'Reilly, A. J. Turberfield, E. Stulz, *Org. Biomol. Chem.* **2011**, *9*, 1661-1666; c) D. Li, X. Wang, F. Shi, R. Sha, N. C. Seeman, J. W. Canary, *Org. Biomol. Chem.* **2014**, *12*, 8823-8827.
[20] V. Patzke, J. S. McCaskill, G. v. Kiedrowski, *Angew. Chem. Int. Ed.* **2014**, *53*, 4222-4226.
[21] a) Y. Meyer, J.-A. Richard, M. Massonneau, P.-Y. Renard, A. Romieu, *Org. Lett.* **2008**, *10*, 1517-1520; b) Y. Meyer, J.-A. Richard, B. Delest, P. Noack, P.-Y. Renard, A. Romieu, *Org. Biomol. Chem.* **2010**, *8*, 1777-1780.
[22] K. Dan, A. T. Veetil, K. Chakraborty, Y. Krishnan, *Nat. Nanotechnol.* **2019**, *14*, 252-259.
[23] Andrew D. Bosson, Jesse R. Zamudio, Phillip A. Sharp, *Mol. Cell* **2014**, *56*, 347-359.
[24] a) X. Chen, N. Briggs, J. R. McLain, A. D. Ellington, *Proceedings of the National Academy of Sciences* **2013**, *110*, 5386-5391; b) D. Y. Zhang, E. Winfree, *Nucleic Acids Res.* **2010**, *38*, 4182-4197.
[25] D. Y. Zhang, A. J. Turberfield, B. Yurke, E. Winfree, *Science* **2007**, *318*, 1121-1125.
[26] S. Mura, J. Nicolas, P. Couvreur, *Nat. Mater.* **2013**, *12*, 991-1003.
[27] a) Q. Xu, G. Zhu, C.-y. Zhang, *Anal. Chem.* **2013**, *85*, 6915-6921; b) L. Wang, W. Li, J. Sun, S.-Y. Zhang, S. Yang, J. Li, J. Li, H.-H. Yang, *Anal. Chem.* **2018**, *90*, 14433-14438.
[28] A. Lacroix, E. Vengut-Climent, D. de Rochambeau, H. F. Sleiman, *ACS Central Science* **2019**, *5*, 882-891.
[29] W. Engelen, S. P. W. Wijnands, M. Merkx, *J. Am. Chem. Soc.* **2018**, *140*, 9758-9767.
[30] J. Zhou, X. Du, N. Yamagata, B. Xu, *J. Am. Chem. Soc.* **2016**, *138*, 3813-3823.

10.1002/anie.202001123

[31] a) X. Tan, B. B. Li, X. Lu, F. Jia, C. Santori, P. Menon, H. Li, B. Zhang, J. J. Zhao, K. Zhang, *J. Am. Chem. Soc.* **2015**, *137*, 6112-6115; b) X. Tan, X. Lu, F. Jia, X. Liu, Y. Sun, J. K. Logan, K. Zhang, *J. Am. Chem. Soc.* **2016**, *138*, 10834-10837; c) C. H. Kapadia, J. R. Melamed, E. S. Day, *BioDrugs* **2018**, *32*, 297-309.

[32] a) J. J. Fakhoury, T. G. Edwardson, J. W. Conway, T. Trinh, F. Khan, M. Barłóg, H. S. Bazzi, H. F. Sleiman, *Nanoscale* **2015**, *7*, 20625-20634; b) T. G. W. Edwardson, K. M. M. Carneiro, C. J. Serpell, H. F. Sleiman, *Angew. Chem. Int. Ed.* **2014**, *53*, 4567-4571; c) D. Bousmail, L. Amrein, J. J. Fakhoury, H. H. Fakih, J. C. C. Hsu, L. Panasci, H. F. Sleiman, *Chemical Science* **2017**, *8*, 6218-6229.

10.1002/anie.202001123

Entry for the Table of Contents

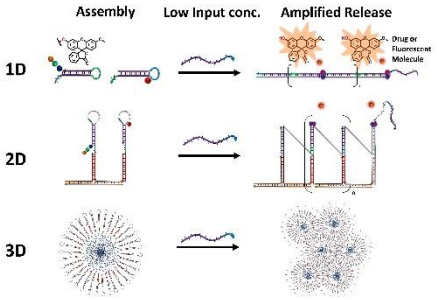

Spatially Isolated and Ready to Amplify: Here, we show the self-immolative, amplified release of small molecules in response to a nucleic acid signal on 1D, 2D, and 3D assemblies using the hybridization chain reaction (HCR). Current methods of small molecule release using a nucleic acid signal rely on reversible hybridization to generate amplification, and as such have not been integrated into standalone nanodevices. We demonstrate the ability of our platforms to effectively separate the reactive groups and subsequently release small molecules in an amplified manner when triggered, for biosensing, imaging and drug delivery.